PHYSICAL REVIEW B **80**, 180505(R) (2009)

Functional renormalization-group study of the doping dependence of pairing symmetry in the iron pnictide superconductors

Ronny Thomale,[1] Christian Platt,[2] Jiangping Hu,[3] Carsten Honerkamp,[2] and B. Andrei Bernevig[4]
[1]*Institut für Theorie der Kondensierten Materie, Universität Karlsruhe, D 76128 Karlsruhe, Germany*
[2]*Theoretical Physics, University of Würzburg, D-97074 Würzburg, Germany*
[3]*Department of Physics, Purdue University, West Lafayette, Indiana 47907, USA*
[4]*Department of Physics, Princeton University, Princeton, New Jersey 08544, USA*
(Received 19 October 2009; published 13 November 2009)

We use the functional renormalization group to analyze the phase diagram of a four-band model for the iron pnictides subject to band interactions with certain A_{1g} momentum dependence. We determine the parameter regimes where an extended s-wave pairing instability with and without nodes emerges. For electron doping, the parameter regime in which a nodal gap appears is in correspondence to recent predictions [A. Chubukov *et al.*, arXiv:0903.5547 (unpublished)], however, at very low T_c. Upon hole doping, the s-wave gap never becomes nodal: above a critical strength of the intraband repulsion, the system favors an exotic extended d-wave instability on the enlarged hole pockets. At half filling, we find that a strong momentum dependence of interband pair hopping yields an extended s-wave instability instead of spin-density wave ordering. These results demonstrate that an interaction anisotropy around the Fermi surfaces generally leads to a pronounced sensitivity of the pairing state on the system parameters.

DOI: 10.1103/PhysRevB.80.180505 PACS number(s): 74.20.Rp, 74.20.Mn, 74.25.Jb, 74.72.Jt

I. INTRODUCTION

The discovery of high-temperature superconductivity in iron-arsenide and related compounds at the beginning of 2008 (Ref. 2) has triggered an enormous interest in condensed-matter physics. This new class of materials exhibits transition temperatures T_c beyond the conventional BCS regime upon electron[3] and hole doping[4] of a collinear antiferromagnetic parent state, with T_c's extending up to 56 K,[5,6] thereby breaking the cuprate monopoly on high-T_c superconductivity.[7]

Various approaches have been pursued to investigate the pairing symmetry in the iron pnictides. By now, after a short period of analysis providing a widespread range of possible pairings,[9–11] an extended s-wave order parameter (denoted $s^{\pm}$ or $s_{x^2y^2}$) that takes opposite signs on the electron and hole pockets along the multiband Fermi surface (FS), emerged with broad theoretical support.[8,12–16] However, experimentally, there is still no broad consensus about the nature of the order parameter. While most experiments can be interpreted in the framework of an $s^{\pm}$ gap,[14] several facts, such as the T^3 dependence of the NMR penetration depth over a significant temperature range, as well as the linear penetration depth in LaOFeP remain unsettled. Other experiments such as penetration depth on the 1111 and 122 compounds, as well as thermal conductivity can be explained by an $s^{\pm}$ order parameter but with large gap anisotropy. Gaps with significant momentum dependence, but no nodes, are reported experimentally in.[17] In contrast, angle resolved photoemission spectroscopy data reveals very isotropic nodeless gaps on the hole Fermi surfaces[18–20] of magnitudes matching a strong-coupling form $\Delta(k)=\Delta_0 \cos(k_x)\cdot\cos(k_y)$ (Ref. 12) in the unfolded Brillouin zone (BZ). Non-nodal gaps have been found in several theoretical approaches to the pnictides.[15,21–24] Functional renormalization-group (fRG) studies[15] with orbital interactions reveal the presence of largely anisotropic, almost nodal, gaps. In the strong-coupling mean-field picture,[12,14] the gap anisotropy is *doping dependent*: the gap has a form $\cos(k_x)\cos(k_y)$ which becomes more anisotropic with increasing doping. In a weak-coupling expansion of FS interactions, it was predicted that the A_{1g} momentum dependence of the interaction along the electron pockets may result in gap anisotropy and possibly nodes on top of the constant $s^{\pm}$ signal.[26,27] A recent random-phase approximation (RPA) analysis on a five-orbital Hubbard model finds a nodal extended s wave.[25]

In this Rapid Communication, we study the influence of interaction anisotropy on the superconducting instability by fRG (Refs. 28–30) methods. We use constant band interactions that only depend on whether the external legs are on hole- or electron pockets. To these we add an A_{1g} momentum dependence in the interband pair hopping interactions g_3 with zero total momentum.[26] For the electron-doped regime, we mostly find non-nodal $s^{\pm}$, where the scale of the gap anisotropy increases with enhanced intraband repulsion g_4. For highly dominant g_4, we indeed find a small parameter regime of nodal $s^{\pm}$. On the hole-doped side, we first find a rather isotropic $s^{\pm}$ signal where the scale of anisotropy does not decisively depend on g_4. Upon further increasing both g_4 and the hole doping, a phase transition occurs, where both the electron and the hole pockets become nodal: the hole pockets develop a d-wave intraband cooper pairing with a sign change on the electron pockets, which we call extended d wave. This clearly demonstrates the possibility of a doping-dependent gap function. Furthermore, we find that strong momentum dependence of g_3 can increase T_c of $s^{\pm}$-wave pairing at half filling such that it even exceeds spin-density wave (SDW) instability, which may relate to recent measurements.[31]

II. FOUR-BAND MODEL

As a model for the band structure, we consider the four-band model of Korshunov and Eremin[22] (see Fig. 1). In the

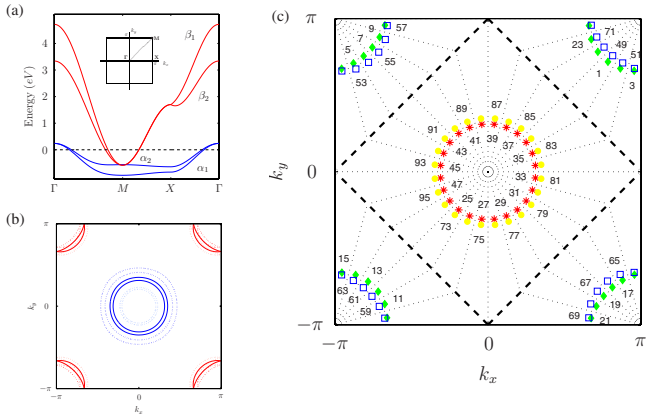

FIG. 1. (Color online) (a) The band structure of the four band model with electron pockets—$\beta_{1,2}$ and hole pocket—$\alpha_{1,2}$. (b) Fermi surfaces at half filling, $x=-.15$ and $x=.15$ doping (c) Illustration of the patching segments in the Brillouin zone.

folded BZ with two Fe ions per unit cell the kinetic Hamiltonian reads as

$$H_0 = -\sum_{\boldsymbol{k},i,\sigma} \epsilon^i n_{\boldsymbol{k}i\sigma} - \sum_{\boldsymbol{k},i,\sigma} t^i_{\boldsymbol{k}} d^\dagger_{\boldsymbol{k}i\sigma} d_{\boldsymbol{k}i\sigma}, \tag{1}$$

where i denotes the band index $i=\alpha_1, \alpha_2, \beta_1, \beta_2$, and the ϵ^i's are on-site energies. The dispersion for the α bands around the Γ point is $t^\alpha_{\boldsymbol{k}}=t^\alpha_1(\cos k_x+\cos k_y)+t^\alpha_2 \cos k_x \cos k_y$, whereas for the β bands around the M point one has $t^\beta_{\boldsymbol{k}}=t^\beta_1(\cos k_x+\cos k_y)+t^\beta_2 \cos k_x/2 \cos k_y/2$. In units of eV and grouped by $(\epsilon^i, t^i_1, t^i_2)$, the parameters take the values $(-0.60, 0.30, 0.24)$ for α_1, $(-0.40, 0.20, 0.24)$ for α_2, (1.70, 1.14, 0.74) for β_1, and $(1.70, 1.14, -0.64)$ for β_2. At half filling, i.e., $\mu=0$, hole and electron pockets are almost perfectly nested.

III. BAND INTERACTIONS

We distinguish four types of band interactions. First, interband couplings depending on whether momentum is transferred within the same band or between the bands,

$$H^{\text{inter}}_I = \sum_{\boldsymbol{k},\boldsymbol{k}',\boldsymbol{q}} g_1 (d^\dagger_{\boldsymbol{k}+\boldsymbol{q}\alpha\sigma} d^\dagger_{\boldsymbol{k}'-\boldsymbol{q}\beta\sigma'} d_{\boldsymbol{k}'\alpha\sigma'} d_{\boldsymbol{k}\beta\sigma} + \text{H.c.}) + g_2 (d^\dagger_{\boldsymbol{k}+\boldsymbol{q}\alpha\sigma} d^\dagger_{\boldsymbol{k}'-\boldsymbol{q}\beta\sigma'} d_{\boldsymbol{k}'\beta\sigma'} d_{\boldsymbol{k}\alpha\sigma} + \text{H.c.}), \tag{2}$$

with implicit sums over σ, σ', and the band indices α and β extending over $\alpha_{1,2}$ and $\beta_{1,2}$, respectively. While g_1 turns out to be rather unimportant for the leading instabilities, g_2 is necessary (but not sufficient) to drive the SDW instability in the (π, π) channel. Furthermore, we consider the interband pair hopping interaction g_3,

$$H^{\text{pair}}_I = \sum_{\boldsymbol{k},\boldsymbol{k}',\boldsymbol{q}} g^b_3 (d^\dagger_{\boldsymbol{k}+\boldsymbol{q}\alpha\sigma} d^\dagger_{\boldsymbol{k}'-\boldsymbol{q}\alpha\sigma'} d_{\boldsymbol{k}'\beta\sigma'} d_{\boldsymbol{k}\beta\sigma} + \text{H.c.}), \tag{3}$$

where, as a central point of our analysis, we add a momentum dependence of the A_{1g}-projected pair hopping amplitude for the zero-momentum Cooper channel:[1]

$$g^b_3|_{\boldsymbol{k}'=-\boldsymbol{k}} = g_3[1+b(\cos k_x + \cos k_y)][1+b(\cos\{k_x+q_x\} + \cos\{k_y+q_y\})], \tag{4}$$

and constant g_3 otherwise. b, the anisotropy scale, gives the relative scale of momentum dependence. To make connection to,[1] g_3 defined in Eq. (4) is given in terms of the unfolded (u) momenta, which relate to the folded (f) ones by $k_{\text{u}\ x,y}=(k_{\text{f}\ x} \pm k_{\text{f}\ y})/2$. Finally, there is the intraband pair interaction

$$H^{\text{intra}}_I = \sum_{\boldsymbol{k},\boldsymbol{k}',\boldsymbol{q}} g_4 d^\dagger_{\boldsymbol{k}+\boldsymbol{q}i\sigma} d^\dagger_{\boldsymbol{k}'-\boldsymbol{q}i\sigma'} d_{\boldsymbol{k}'i\sigma'} d_{\boldsymbol{k}i\sigma}, \tag{5}$$

where i extends over all band indices. For H^{pair}_I in the total zero-momentum Cooper channel, one Cooper pair belongs to the electron pockets and the other one to the hole pockets, rendering g_3 to significantly deviate depending on the momenta along the electron FS, but gives only a constant value $g_3 \approx 1+2b$ on the hole pockets.

IV. *f*RG METHOD

We use the fRG method to study the flow of the two-particle vertex function $V^\Lambda(\boldsymbol{k}_1, a, \boldsymbol{k}_2, b, \boldsymbol{k}_3, c, \boldsymbol{k}_4, d)$, where $\boldsymbol{k}_{1,2}(\boldsymbol{k}_{3,4})$ denote the ingoing (outgoing) particles, $a, \ldots, d$ are the different band indices, and Λ is the energy cutoff above which the high energy modes have been integrated out and incorporated into the effective vertex function. The expression "function" comes from the functional dependence of V on the ingoing and outgoing momenta, while the value of k is discretized to different patches, as explained above. Details on the implementation for the multiband case of pnictides can be reviewed in Refs. 15 and 21. While $\boldsymbol{k}_4$ is implicitly given by momentum conservation, the spin convention is that $\boldsymbol{k}_1(\boldsymbol{k}_2)$ and $\boldsymbol{k}_3(\boldsymbol{k}_4)$ have the same spin.

To solve the RG equations numerically, the momenta in the BZ are discretized as shown in Fig. 1. We find that $N=96$ both provide sufficient resolution and suitable computation time performance for our studies. Essentially, the RG flow in terms of the cutoff parameter Λ starts at cutoff energies of the order of the bandwidth, and successively decreases toward the FS. In each differential step, both particle-particle and particle-hole contributions influence the evolution of the coupling function. Quite generically, these flows lead to strong coupling, i.e., one or more channels in the vertex function flow to large absolute values at a critical scale Λ_c. This scale provides a reasonable estimate of actual critical temperatures T_c for phase transitions when long-range ordering is possible.

V. ELECTRON DOPING

First we want to specify the parameter window where nodal and non-nodal $s^\pm$ appears for electron doping ($x=0.2$). We consider the case of $g_1=0.1$ and $g_2=0.25$, and choose $g_3=0.3$ to be of the order of g_2 (throughout the article, the interaction couplings are given in units of eV where the total bandwidth is ~ 6 eV). The g_3 anisotropy scale b and $\gamma=g_4/g_3$ span the relevant parameter space of interactions and allow for nodal gaps according to Ref. 1. For elec-

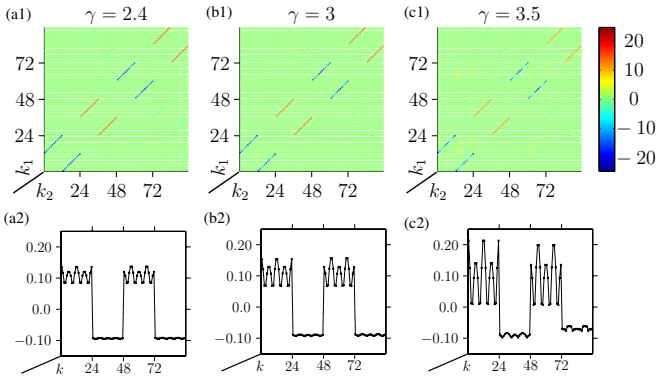

FIG. 2. (Color online) (a1)–(c1) Plot of the vertex function vs incoming momenta for $g_1=0.1$, $g_2=0.25$, $g_3=0.3$, $g_4=\gamma g_3$, $b=1.1$, and γ varied as 2.4, 3, and 3.5 from left to right. k_4 is fixed by total momentum, k_3 is chosen on patch sector 55. As indicated by the scale in the plot of the upper line, the vertex function takes on values of generally different absolute value and sign. Upon increase in γ, one clearly observes the nodal structure on the electron pockets to become more pronounced, while the hole pockets show a homogeneously diverging vertex without anisotropy. (a2)–(c2) Plot of the associated superconducting form factor. The signal along the hole pockets is constant; nodal peaks slowly develop on the electron pockets.

tron doping, the pockets nesting is lifted and the SDW instability is suppressed. For $b \ll 1$, one finds a constant $s^{\pm}$ instability, as observed in Ref. 21, whose critical scale Λ_c decreases with increasing γ. The $s^{\pm}$ instability manifests itself as a Cooper instability corresponding to a divergent vertex for $\boldsymbol{k}_1=-\boldsymbol{k}_2$, with a sign change of the vertex going from electron to hole pockets, as it can be seen both in the vertex plot and the form factors in Fig. 2. Upon increasing b, Λ_c increases considerably and helps to counteract the intraband repulsion g_4. In addition, a gap variation starts to emerge on the electron pockets, while the hole pockets remain unchanged. In particular, the gap anisotropy increases upon increasing γ, which shows that the system favors a nodal variation to compensate the increasing intraband repulsion g_4, as predicted in Ref. 1. However, for $\gamma \lesssim 3$, this anisotropy never becomes comparable to the constant gap scale on the electron pockets; i.e., the nodes do not completely develop. Upon increasing $\gamma > 3$, the gap variation in the electron pockets gets more pronounced to finally yield a nodal extended s-wave instability [Fig. 2(c)]. Taking into account the rescaling conventions of u_3 as it appears in the Rapid Communication, this is in approximate correspondence with Ref. 1. Increasing b even further at constant γ, $g_3 \approx 1+2b$ on the hole pockets is considerably enhanced and leads to a reduction in gap anisotropy on the electron pockets (see Figs. 2 and 4).

VI. HOLE DOPING

We now consider hole doping with the same interaction parameters $g_1=0.1$, $g_2=0.25$, and $g_3=0.3$. For small anisotropy b, the system likewise develops a rather constant $s^{\pm}$ instability, where T_c decreases with γ. For considerable values of b and a ratio γ as for electron doping, the hole-doped scenario still favors a constant $s^{\pm}$ instability (Fig. 3). Unlike in the electron-doped case, increasing γ does not immediately induce gap anisotropy on the electron pockets: the only result (mostly) is a decreasing gap on the hole Fermi surfaces. This behavior can be explained due to the small electron FS size: for hole doping, the hole FSs dominate the behavior of the system. The A_{1g} term induces anisotropy mostly on the electron FSs, which at hole doping are rather small. On the hole pockets, the A_{1g} term increases the size of the constant part of the interaction g_3, which favors an $s^{\pm}$. This, coupled to the fact that the electron FSs play a rather secondary role compared to their hole counterparts, renders the symmetry to be $s^{\pm}$ for moderate γ. Increased γ has the effect of reducing the scale of the superconducting instability. While in the electron-doped case, increasing γ resulted in nodal electron FSs (while keeping the hole FSs isotropic nodeless), for hole doping, the situation is completely different. Beyond a critical γ, when the $s^{\pm}$ gaps have vanished, the system exhibits a phase transition with nodal superconductivity on *both* hole and electron FSs. For $\gamma \gtrsim 2.4$, at comparably low transition temperature, the leading instability becomes a d-wave intraband Cooper pairing on the hole pockets. This is plausible from the FS topology upon doping as shown in Fig. 1(b): the hole FS's around Γ grow significantly upon hole doping. For dominant intraband repulsion g_4, the favorable ordering becomes a d-wave Cooper pairing on the hole pockets, as shown in Fig. 3. In terms of the hole FS only, this is a situation similar to the cuprates. We also find a small d-wave type signal on the electron pockets, which relates to the d-wave signal on the hole pockets shifted by π: there is still an overall sign change between the gaps on hole and electron pockets. In this way, the system minimizes both intra- and interband repulsions: this is the d-wave equivalent of the $s^{\pm}$ instability, which one may denote extended $d^{\pm}$-wave (Fig. 3(c)). While interesting in its own right, the phase diagram on the hole-doped side does not allow for a nodal electron FS *while* keeping the hole FS fully

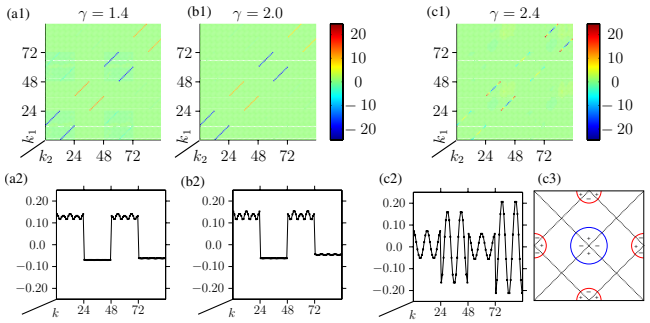

FIG. 3. (Color online) (a1)–(c1) Plot of the vertex function with interband interaction $g_1=0.1$, $g_2=0.25$, $g_3=0.3$, $g_4=\gamma g_3$, $\gamma=2.4$, $b=1.1$, $x=-0.18$, and $\gamma=1.4, 2.0, 2.4$. The scale in the upper line similarly signal sign and absolute value of the vertex function as in Fig. 2. For (a1) and (b2) we observe an ordinary $s^{\pm}$ instability with small gap variation as shown in the form factor (a2) and (b2). In (c1), we observe a leading signal on the hole pockets originating from a d-wave pairing, where the nodes can be seen in the form factor (c2). (c3) gives a visualization of the extended d-wave state in the unfolded Brillouin zone.

gapped. We conclude that an A_{1g} symmetry term alone is not sufficient to make the electron FS nodal while keeping the hole FS fully gapped at both electron and hole doping.

VII. FULL PHASE DIAGRAM AND INTERPLAY OF SDW AND $s^{\pm}$ AT HALF FILLING

For all settings discussed above, we find a leading SDW instability as we approach half filling, as the SDW benefits from the nesting of hole and electron pockets. Now, upon increasing b from 1.5 to 1.8, the $s^{\pm}$ pairing instability becomes dominant over the SDW and becomes the leading instability even at half filling. The b_c where this occurs increases with γ. Interestingly, the critical scale is not suppressed between the two regimes which in a less approximate treatment would be most likely separated by a first-order transition. Hence, a slight change in the system parameters can turn the system from a high-scale SDW into a $s^{\pm}$ state with comparable pairing scale—another possibility for a marked material dependence of the phase diagrams of pnictides. In fact, the finding of a leading $s^{\pm}$ instability at half filling may relate to present experiments where a superconducting state was found even in a parent compound without doping.[31] The full phase diagram for two representative interaction settings is given in Fig. 4.

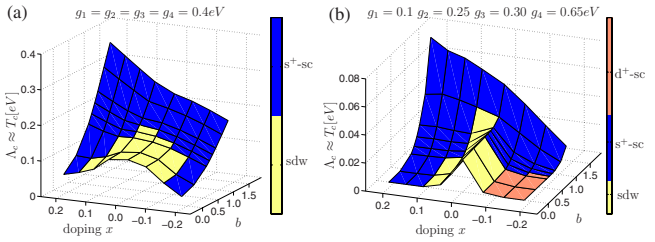

FIG. 4. (Color online) Phase diagrams for different interaction settings, (a) $g_1=g_2=g_3=g_4=0.4$ and (b) $g_1=0.1$, $g_2=0.25$, $g_3=0.3$, $g_4=\gamma$ $g_3=0.65$. The three axes are given by the filling factor x, momentum anisotropy b and the critical temperature T_c. (a) In a dome around half filling, the SDW instability is leading. It is overcome by the superconducting instability at higher b and electron (hole) doping. T_c increases with b, in particular on the electron-doped side. (b) γ is increased. The SDW dome shrinks in doping width but increases on the anisotropy line as the superconducting T_c is decreased due to g_4. For hole doping at small b, we observe nodal $d^{\pm}$. $s^{\pm}$ gap variation on the electron-doped side is enhanced, while true nodal extended s wave is successively observed on the electron pockets only for even larger $\gamma \approx 3$.

VIII. CONCLUSION

We studied the effect of a certain momentum dependence of the band interactions in a four-band model of the pnictides. Increasing intraband repulsion enhances the $s^{\pm}$ gap anisotropy on the electron pockets, which may ultimately, but not easily, lead to a true nodal electron FS gap. For the hole-doped regime, however, the gap anisotropy always remains rather small even on the electron FS, up to a critical value of the intraband repulsion beyond which the system favors an exotic and sign-reversed d-wave signal on the hole and electron pockets. We are unable to find a regime which satisfies the conditions of having gapped hole FS and nodal electron FS for *both* electron and hole doping.

ACKNOWLEDGMENTS

We thank M. Eschrig, W. Hanke, D.-H. Lee, F. Wang, P. Wölfle, and S. C. Zhang for discussions. C.H. and C.P. acknowledge support from DFG (Grants No. DFG-FOR538 and No. FOR723), and B.A.B. from the Alfred P. Sloan Foundation.

[1] A. Chubukov *et al.*, arXiv:0903.5547 (unpublished).
[2] Y. Kamihara *et al.*, J. Am. Chem. Soc. **130**, 3296 (2008).
[3] G. F. Chen *et al.*, Phys. Rev. Lett. **100**, 247002 (2008).
[4] M. Rotter *et al.*, Phys. Rev. Lett. **101**, 107006 (2008).
[5] X. H. Chen *et al.*, Nature (London) **453**, 761 (2008).
[6] C. Wang *et al.*, EPL **83**, 67006 (2008).
[7] E. Berg *et al.*, arXiv:0905.1096 (unpublished).
[8] K. Kuroki *et al.*, Phys. Rev. Lett. **101**, 087004 (2008).
[9] Q. Si and E. Abrahams, Phys. Rev. Lett. **101**, 076401 (2008).
[10] P. A. Lee and X.-G. Wen, Phys. Rev. B **78**, 144517 (2008).
[11] X. Dai *et al.*, Phys. Rev. Lett. **101**, 057008 (2008).
[12] K. Seo *et al.*, Phys. Rev. Lett. **101**, 206404 (2008).
[13] I. I. Mazin *et al.*, Phys. Rev. Lett. **101**, 057003 (2008).
[14] M. M. Parish *et al.*, Phys. Rev. B **78**, 144514 (2008).
[15] F. Wang *et al.*, Phys. Rev. Lett. **102**, 047005 (2009).
[16] V. Cvetkovic and Z. Tesanovic, EPL **85**, 37002 (2009).
[17] T. Kondo *et al.*, Phys. Rev. Lett. **101**, 147003 (2008).
[18] L. Wray *et al.*, Phys. Rev. B **78**, 184508 (2008).
[19] A. Koitzsch *et al.*, Phys. Rev. B **78**, 180506(R) (2008).
[20] H. Liu *et al.*, Phys. Rev. B **78**, 184514 (2008).
[21] C. Platt *et al.*, New J. Phys. **11**, 055058 (2009).
[22] M. M. Korshunov and I. Eremin, Phys. Rev. B **78**, 140509(R) (2008).
[23] A. V. Chubukov *et al.*, Phys. Rev. B **78**, 134512 (2008).
[24] V. Stanev *et al.*, Phys. Rev. B **78**, 184509 (2008).
[25] S. Graser *et al.*, New J. Phys. **11**, 025016 (2009).
[26] A. Chubukov, Physica C **469**, 640 (2009).
[27] T. Maier *et al.*, Phys. Rev. B **79**, 224510 (2009).
[28] R. Shankar, Rev. Mod. Phys. **66**, 129 (1994).
[29] C. Honerkamp *et al.*, Phys. Rev. B **63**, 035109 (2001).
[30] C. J. Halboth and W. Metzner, Phys. Rev. B **61**, 7364 (2000).
[31] X. Zhu *et al.*, Phys. Rev. B **79**, 220512(R) (2009).